Gene transfer of two entry inhibitors protects CD4+ T cell from HIV-1 infection in humanized mice

N y Petit, C Baillou, A Burlion, K Dorgham, B Levacher, C Amiel, V Schneider, F M Lemoine, G Gorochov, Gilles Marodon

Gene transfer of two entry inhibitors protects CD4$^+$ T cell from HIV-1 infection in humanized mice

- Running title: HIV-1 gene therapy in humanized mice

Nicolas Y. Petit[1], Claude Baillou[1], Aude Burlion[1], Karim Dorgham[1], Béatrice Levacher[2], Corinne Amiel[1,3], Véronique Schneider[3], François M. Lemoine[1], Guy Gorochov[1,4], Gilles Marodon[1]

[1] Sorbonne Universités, UPMC Univ PARIS 06, CR7, INSERM U1135, CNRS, Centre d'Immunologie et des Maladies Infectieuses (CIMI), Paris, France

[2] Sorbonne Universités, UPMC Univ PARIS 06, CR7, INSERM U959, Paris, France

[3] AP-HP, Hôpital Tenon, Service de Virologie, Paris, France

[4] AP-HP, Hôpital Pitié-Salpêtrière, Département d'Immunologie, Paris, France

- The authors declare no conflict of interest.

- Corresponding author address: CIMI-PARIS, Bât CERVI, Hôpital Universitaire Pitié-Salpêtrière, 83 Bd de l'Hôpital, 75013 PARIS, FRANCE, tel:+33 14 217 7468 Fax: +33 217 7462, email: gilles.marodon@upmc.fr

This work was supported by grants from Agence Nationale de la Recherche to Guy Gorochov and Gilles Marodon. Nicolas Petit was supported by a doctoral fellowship from Fond Pierre Bergé /SIDAction and by the ANRS.

Abstract

Targeting viral entry is the most likely gene therapy strategy to succeed in protecting the immune system from pathogenic HIV-1 infection. Here, we evaluated the efficacy of a gene transfer lentiviral vector expressing a combination of viral entry inhibitors, the C46 peptide (an inhibitor of viral fusion) and the P2-CCL5 intrakine (a modulator of CCR5 expression), to prevent $CD4^+$ T cell depletion *in vivo*. For this, we used two different models of HIV-1-infected mice, one in which *ex vivo* genetically-modified human T cells were grafted into immunodeficient NOD.SCID.$\gamma c^{-/-}$ mice before infection and one in which genetically-modified T cells were derived from $CD34^+$ hematopoietic progenitors grafted few days after birth. Expression of the transgenes conferred a major selective advantage to genetically-modified $CD4^+$ T cells, the frequency of which could increase from 10 to 90% in the blood following HIV-1 infection. Moreover, these cells resisted HIV-1-induced depletion, contrary to non-modified cells that were depleted in the same mice. Finally, we report lower normalized viral loads in mice having received genetically-modified progenitors. Altogether, our study documents that targeting viral entry *in vivo* is a promising avenue for the future of HIV-1 gene therapy in humans.

Introduction

Although there is no consensus on a definitive immune correlate of protection, there are multiple convincing examples linking human genetics and susceptibility to HIV-1 infection. The best example of a genetic predisposition protecting from HIV-1 remains the Δ32 mutation that prevents CCR5 expression at the cell surface, and thus completely protects 1% of Europeans from being infected. [1] The so-called 'Berlin patient' was grafted with CCR5-deficient bone marrow to treat his leukemia and was subsequently cured of both diseases. [3] Simultaneously, genetic interventions targeting chemokine receptors using DNA -nucleases gave encouraging results in humanized mice (HuMice) [3–5] but the long term impact of this procedure, as well as the concerns with off-target cleavages, is still unknown. Clinical trials applying this strategy to lymphocytes or stem cells have shown that modified cells possessed a selective advantage compared with non-modified cells, [6] which is one criterion of success for the therapy. Thus, there is a strong rationale to use gene therapy as an adjunct to current and future treatments. [7]

Maraviroc, a CCR5 chemical antagonist, is a powerful medication *in vitro* but resistant variants rapidly emerge in treated patients for complex reasons, such as mutations in the gp120 coding sequence affecting CCR5 docking. [8] Similarly, the fusion inhibitor Enfuvirtide (a gp41 analog), which is delivered in solution to patients, rapidly becomes ineffective because gp41 mutates to escape Enfuvirtide binding. [9] Thus, the therapeutic arsenal targeting viral entry is scarce and poorly efficient. However, strategies based on blocking entry are perhaps the most promising to rapidly restore a pool of functional T cells, the main goal to prevent AIDS. [10] More recently, it was shown that HIV-1 infection needs not to be productive in $CD4^+$ T cells to induce

cell death by pyroptosis [11]. This mechanism of HIV-1-induced cell death highlights the interest of strategies aimed at preventing viral entry. We proposed developing a gene transfer vector in which two viral entry inhibitors in combination would have a better efficacy at preventing viral entry. In support of this hypothesis, a synergistic effect of Enfuvirtide was demonstrated in cells with low levels of CCR5 [12]. Importantly, viral variants able to escape gp41 analogs and CCR5 inhibitors at the same time have only been described *in vitro* with a drastic cost on viral fitness, [13] illustrating the difficulty for the virus to escape both inhibitors at the same time. Using monocistronic lentiviral vectors, we previously showed a synergistic effect of the P2-CCL5 intrakine with the C46 peptide on HIV-1 infection *in vitro* [14]. The P2-CCL5 intrakine, originally described as a high affinity CCL5 (RANTES) variant, [15] was later modified to incorporate an ER retention sequence, sequestering CCR5 away from the cell surface [16]. The C46 peptide is the optimized membrane-bound form of Enfuvirtide and has been used in several gene therapy studies since it is effective on both CCR5- or CXCR4-tropic HIV-1, and can be accommodated in several gene transfer vectors, including lentiviral vectors [17–20]. Here, we aimed to evaluate the *in vivo* efficacy of an optimized lentiviral vector co-expressing those two entry inhibitors. We used two pre-clinical models of HIV-1 gene therapy, either infusing genetically-modified T cells in adult immunocompromised NOD.SCID.gc$^{-/-}$ (NSG/PBL) mice or grafting genetically-modified hematopoietic progenitors in NSG neonates (NSG/CD34).

Results

A lentiviral vector expressing two inhibitors of HIV-1 entry

With the general aim to validate the combination of the C46 peptide and the P2-CCL5 intrakine for HIV-1 gene therapy *in vivo*, we used an optimized version of our previously described lentiviral vector, which efficiently inhibited HIV-1 infection *in vitro.*[14] To facilitate detection of genetically-modified cells, we added the GFP reporter gene after the therapeutic cassette to generate the LvGFP-C46-P2 vector (Fig. 1a). A vector using the same strong promoter EF1α but in which the therapeutic cassette was omitted was used as a control (Fig. 1a). We transduced anti-CD3/CD28 activated PBMCs to monitor transgene expression and function *in vitro* and *in vivo*. Expression of the GFP reporter molecule was well correlated with the expression of the C46 peptide (detected with the 2F5 monoclonal antibody) (Fig. 1b) and was also associated with a lower median fluorescence intensity (MFI) of CCR5 *in vitro* (Fig. 1c). Passive diffusion of the intrakine was ruled out by the observation that GFP^- cells exhibited similar CCR5 MFI than non-transduced cells (Fig. 1c), suggesting that this reduction was due to ER retention of CCR5 through interaction with the P2-CCL5 intrakine.. The MFI of CCR5 was also reduced two-fold in genetically-modified PBMCs injected *in vivo* in NSG mice (Fig. 1d), reflecting the expected down-modulation of CCR5 surface expression. Thus, GFP expression was a faithful reporter of transgenes expression and function, and was thus used to follow genetically-modified cells *in vivo*.

Protection of genetically-modified human CD4$^+$ T cells from HIV-1 infection in NSG/PBL mice

As a model for HIV-1 infection of human CD4$^+$ T cells *in vivo*, we first used adoptive cell transfer (ACT) in immunocompromised NSG mice (NSG/PBL). A major problem with ACT of human T cells in NSG mice is the xenogeneic graft-versus-host disease (GVHD) that develops thereafter and that invariably leads to death.[21] We tested various ACT protocols in NSG mice and found that injection of 6.10^6 activated T cells in 1 Gy-irradiated mice represented an optimal trade-off between survival and engraftment efficiency (protocol P3 in Figure S1). To normalize the number of genetically-modified cells across experiments and vectors, we diluted transduced cells into non-transduced cells *ex vivo* prior ACT, establishing a number of GFP$^+$ cells at 10% of the injected cells. Mice were infected i.v with a CCR5-tropic HIV-1 strain 12 days after ACT. The frequencies of CD4$^+$GFP$^+$ cells steadily increased in the blood of LvGFP-C46-P2-treated animals during the course of the infection to reach a plateau where up to 95% of all CD4$^+$ T cells expressed the transgene (Fig. 2a). In contrast, the frequencies of GFP$^+$ cells in control HIV-1-infected LvGFP-treated mice remained close to the 10% input throughout the experiment (Fig. 2a). The increase in GFP$^+$ cells with the LvGFP-C46-P2 vector was dependent on HIV-1 infection because it was not observed in non-infected NSG/PBL mice (Fig. S2), showing that the therapeutic vector did not increase the proliferation of modified cells *per se*. The frequencies of GFP$^+$ cells were also superior in the spleen and in the bone marrow of LvGFP-C46-P2-treated mice compared with LvGFP-treated control mice (Fig. 2b). These increased frequencies translated into increased numbers of CD4$^+$GFP$^+$ cell in the spleen and the bone marrow of

LvGFP-C46-P2-treated mice compared with LvGFP mice (Fig. S3). Altogether, the results demonstrate that LvGFP-C46-P2-transduced $CD4^+$ T cells possess a selective advantage relative to LvGFP-modified T cells.

To test the hypothesis that genetically-modified cells resisted HIV-1-induced depletion, we analyzed longitudinally the frequencies of $CD4^+$ cells in $CD3^+GFP^+$ and $CD3^+GFP^-$ T cells in the blood of LvGFP-C46-P2- and LvGFP-treated mice (Fig. 2c). The frequencies of $CD4^+$ T cells in the GFP^- subset rapidly dropped after HIV-1 infection, showing that non-protected $CD4^+$ T cells underwent HIV-1-induced depletion as expected (Fig. 2d). In striking contrast, the frequency of $CD4^+$ T cells in the GFP^+ fraction remained constant throughout the experiment, showing that these cells were protected from HIV-1-induced depletion. Resistance to depletion was also observed in the spleen and in the bone marrow of LvGFP-C46-P2-treated animals, with statistically significant differences in the frequencies of $CD4^+$ T cells in GFP^+ vs GFP^- T cells (Fig. 2e). In contrast, the frequencies of GFP^+ cells, like the GFP^- subset, steadily decreased in the blood of control LvGFP-treated mice (Fig. S4a), showing that GFP expression *per se* did not protect from HIV-1-induced deletion. A similar depletion of GFP^+ cells were found in the spleen and in the bone marrow of control LvGFP-treated mice (Fig. S4b). Thus, $CD4^+$ T cells expressing the combination of viral entry inhibitors were protected from HIV-1-induced depletion in NSG/PBL mice in the blood and in lymphoid tissues.

Resistance of genetically-modified human $CD4^+$ T cells to HIV-1-induced depletion in NSG/CD34 HuMice

We next wanted to confirm the potency of the vector to prevent HIV-1-induced $CD4^+$ T cell depletion in a more physiological setting. For this, we grafted LvGFP-C46-P2-transduced CD34-purified cells from cord blood into neonatal NSG mice and monitored human cell reconstitution and transgene expression overtime. At 17 weeks post-injection, 11.9 ± 11.0 % of total cells from the blood (excluding erythrocytes) were human $CD45^+CD3^+$ T cells in the animals used for the experiment. The frequencies of $CD4^+$ and $CD8^+$ T cells among $CD3^+$ cells were less variable representing 40.0 ± 5.8 % and 47.0 ± 5.3 % , respectively (Fig. S5). Among 14 NSG/CD34 HuMice generated with LvGFP-C46-P2-modified $CD34^+$ cells, only 8 had detectable GFP^+ cells in $CD4^+$ T cells 17 weeks after. Four of those mice were infected with a CCR5-tropic HIV-1 strain, whereas 4 were left uninfected. Because the frequency of GFP^+ cells was highly variable among NSG/CD34 HuMice, it was not possible to reliably measure a selective advantage in that setting. To directly assess resistance of genetically-modified $CD4^+$ T cells to HIV-1-induced depletion, frequencies of $CD4^+$ T cells were measured in GFP^+ and GFP^- cells (Fig. 3). In non-infected mice, the frequencies of $CD4^+$ T cells in the blood remained similar in GFP^+ vs GFP^- T cells throughout the course of the experiment (Fig. 3a). As expected, frequencies of GFP^- cells steadily decreased in HIV-1-infected animals whereas frequencies of GFP^+ remained stable, showing that $CD4^+GFP^+$ T cells resisted HIV-1-induced depletion in the blood of NSG/CD34 HuMice (Fig. 3b). As expected in non-infected mice, the frequencies of $CD4^+$ T cells in lymphoid organs were similar in GFP^+ or GFP^- subsets (Fig. 3c). In contrast, frequencies of $CD4^+$ T cells among GFP^+ and GFP^- cells significantly differed in the LN, spleen and bone marrow (Fig. 3d). Of note is the one mouse in which resistance to deletion was not evident in the blood did not show any sign of resistance in the lymphoid organs. Thus, gene transfer of two

entry inhibitors in $CD34^+$ cells conferred resistance to $CD4^+$ T cells in 3 mice out of 4 analyzed.

Gene transfer of entry inhibitors impact viral replication in NSG/CD34 HuMice.

To assess the impact that the therapy might have on viral loads, we measured viremia in LvGFP-C46-P2-treated mice in which GFP^+ cells were observed (n=4) or not (n=6) prior HIV-1 infection. To accommodate the various levels of human cells engrafment among the different mice (Fig. S5), viremia was corrected by the frequency of $CD45^+CD3^+CD4^+$ T cells among total cells of the blood at the time of the analysis. Initially, normalized viremia was similar in both groups, showing that the therapy was not associated with an immediate effect on viral replication. However, we observed a tendency for lower normalized viral loads in mice bearing GFP^+ cells compared to mice in which no GFP^+ cells could be detected (Fig. 4a). To confirm that animals with GFP^+ cells carried less virus, we analyzed p24 expression in $CD4^+$ T cells at the end of the experiment. We found that the frequencies of $CD4^+$ cells expressing p24 in mice with GFP^+ cells were lower than in mice without GFP^+ cells and close to background staining obtained in non-infected HuMice (Fig. 4b). Altogether, we conclude that NSG/CD34 HuMice reconstituted with gene-modified $CD34^+$ progenitors were protected from HIV-1-induced $CD4^+$ T cell deletion and had a lower number of infected cells, corroborating with lower viral loads.

Discussion

Here, we show that a lentiviral vector encoding two viral entry inhibitors confers a selective advantage to genetically-modified cells *in vivo*, due to their resistance to HIV-1-mediated depletion. We observed a strong and long-lasting selective advantage in the NSG/PBL model. A lower selective advantage was reported in a very similar model of NSG/PBL HuMice using a vector expressing only the C46 peptide. [18] This observation suggest that two entry inhibitors might be better than one at protecting cells from HIV-1. However, a pre-clinical study in macaques reconstituted with progenitors expressing the C46 peptide alone showed lower viral loads correlated to a clear selective advantage [22]. Moreover, recent studies showed that inhibition of CCR5 expression by shRNA was sufficient to protect $CD4^+$ T cells from infection and to confer a selective advantage in chimeric Bone marrow-Liver-Thymus (BLT) HuMice [23,24]. Thus, targeting gp41 and CCR5 have independently the potential to curb HIV-1 infection, highlighting the interest of using two inhibitors of this crucial step of HIV-1 infection in the same vector.

A strong selective advantage is not always associated with lower viral loads. In CD34-reconstituted HuMice, Walker et al. reported that expression of a triple combination of anti-HIV-1 genes did not impact viral replication, although a significant selective advantage was observed. [25] A modest but significant effect on viral loads was reported following CCR5-specific ZFN-mediated modification in NSG/PBL HuMice. [5] However, only one time point was analyzed in that study. A kinetics study showed that the reduction in viral loads using the same technology was much more discrete in NSG/CD34 HuMice despite a considerable selective advantage. [3] Our PCR and p24 data concur to the hypothesis that selective advantage conferred by our vector had

an impact on viral replication. Recently, a complete protection from HIV-1 was observed in BLT mice reconstituted with human cells modified with a vector very similar to our, encoding the C46 peptide and a shRNA targeting CCR5 [19]. This is the first report showing that viral replication can be totally controlled in humanized mice by gene therapy without prior sorting of genetically-modified cells, as recently shown for a CCR5 shRNA [26]. This surprising and unique result suggest that maximal efficacy of HIV-1 gene therapy might necessitate a functional immune response, that is present in monkeys and BLT HuMice but lacking or severely hampered in other HuMice models. One must keep in mind though that some HIV-1-specific PCR might amplify the vector as well [27]. The use of HIV-1-specific PCR discriminating HIV-1 from the vector such as the one employed in our study should become the gold standard.

Considering the recent developments of nucleases that target CCR5 in $CD34^+$ progenitor cells , we believe that residual expression of the molecule such as the one observed with our intrakine, might allow for normal hematopoeisis and circulation of modified-cells while total ablation by genetic means may impact on these processes. Recent advances in lentiviral delivery of ZN finger nucleases might improve specific targeting of the nuclease to mature $CD4^+$ T cells, a protocol that would limit bystander effects [28].

The selective advantage of genetically-modified cells would only be obtained in the context of high levels of viral replication. Although ART interruptions have been performed in the past to provoke selective growth of modified cells in small-scale clinical trials for gene therapy, [29,30] an interruption in therapy is not foreseeable in patients in the long term. Gene therapy might thus be particularly suitable for patients experimenting treatment failure with high viral loads.

Materials and Methods

Lentiviral vector design and production

Second-generation self-inactivating (SIN) lentiviral vectors were used in this study. [31] The LvGFP-C46-P2 vector was constructed by adding an eGFP gene and 2A sequence upstream of the therapeutic cassette (construction encoding the C46 peptide and P2-CCL5 analog described in Petit et al., 2014) [14] in the backbone of a lentiviral vector carrying the EF1a promoter. As a control, the LvGFP vector expressing GFP only was used. Details on the cloning procedures are available on request. Lentiviral vectors were produced in mycoplasma-free HEK-293T cells, as described previously. [32] Briefly, 23.3 µg of the Δ8.9 packaging plasmid, 30 µg of the vector plasmid, and 10 µg of the vesicular stomatitis virus (VSV)-G envelope were transfected into 15.10^6 cells in T-175 flasks by calcium phosphate precipitation. Vector supernatants were collected 48 hours post-transfection and concentrated by ultrafiltration (Centricon Plus-70; Millipore, Molsheim, France) at 3500 g at 4°C. Viral stocks were kept frozen at -80° C. Viral titers were determined on HEK-293T cells with various concentrations of vector supernatants in the presence of Polybrene (8 µg/mL; Sigma-Aldrich, Saint-Quentin-Fallavier, France). Seventy-two hours after transduction, the percentage of cells expressing the transgenes was determined by flow cytometry and used to calculate a viral titer as the number of infectious particles per milliliter.

Mice and humanization

NOD Prkdc^{scid} Il2rg^{tm1Wjl} (NSG) mice (strain ≠05557; Jackson Laboratory, USA) were bred in animal facilities of Centre d'Expérimentation Fonctionnelle (CEF) according to the Jackson Laboratory handling practice specific to that strain. The regional ethical committee on animal experimentation Darwin approved all mouse protocols. Primary human cells were obtained from leukapheresis samples collected from healthy donors at the Etablissement Francais du Sang after informed consent. Cells were grown at a concentration of 1.10^6 cells/mL and activated in RPMI, 10% FCS, penicillin/streptomycin, interleukin-2 (Proleukin, 600 IU/mL; Novartis, Basel, Switzerland), and CD3/CD28 beads (Invitrogen, Carlsbad, CA) at 3 beads per cell. Two days after activation, cells were transduced by spinoculation for 2 hrs at 1000 g at 30°C, with the indicated lentiviral vectors at a multiplicity of infection (MOI) of 6 to 8 in the presence of protamine sulfate (2 µg/mL, Sigma). Three days after transduction, 1 Gy-irradiated female 8 to 12-weeks old NSG mice were injected with 6.10^6 cells. Twelve days post-adoptive cell transfer (ACT), mice were infected with 25 ng of p24 of NLAD8 HIV-1 strain in a final volume of 100 µL of 1X PBS. All mice used in this study were randomly assigned to experimental group and cages. Investigator was not blinded to the group allocation during the experiments.

Human hematopoietic progenitor cells were obtained from cord blood samples collected from healthy donors after informed consent. Mononuclear cells from human cord blood were isolated by Ficoll density gradient and centrifuged at 200 g during 13 min to remove platelets. Then, $CD34^+$ progenitors were sorted with the human CD34 MicroBeads kit, according to the manufacturer's instructions (Miltenyi). $CD34^+$ cells were incubated at a concentration of 1.10^6 cells/mL over night into StemSpan SFEMII medium (StemCell technologies) complemented with

human recombinant cytokines (IL-6 and TPO at 20 ng/mL; SCF and FLT3-L at 100 ng/mL; Peprotech) and antibiotics. Cells were transduced with the LvGFP-C46-P2 lentiviral vector in StemSpan medium in the presence of cytokines, the proteasome inhibitor MG-132 (1 µM; Sigma), antibiotics and protamine sulfate (8 µg/mL; Sigma). $CD34^+$ cells underwent two rounds of transduction separated by 3 hours incubation at 37°C and 5% CO_2. For each transduction cycle, cells were centrifuged at 1000 g at 30°C for 2 hours with the lentiviral vector at a MOI of 15. Twenty-four to 48-hour-old NSG mice were irradiated at 0.9 Gy and grafted with $0.5.10^5$ to $2.5.10^5$ transduced $CD34^+$ cells by the intra-hepatic route. Ten ng of the p24 NL-AD8 HIV-1 strain were injected into the retro-orbital sinus of 17 weeks-old mice in a final volume of 100 µL of 1X PBS.

HIV-1 production and quantification

HIV-1 molecular clone NL-AD8 was obtained through the AIDS Research and Reference Reagent Program. HIV-1 stocks were prepared with 30 µg of plasmid transfected into 15.10^6 mycoplasma-free HEK 293T cells in T-175 flasks by calcium phosphate precipitation. The supernatant was frozen at -80°C and viral titers were quantified by p24 ELISA according to the manufacturer's instructions (Zeptometrix, Buffalo, NY). Mice were bled on ACD (acid-Citrate-Dextrose) anticoagulant and plasma HIV-1 RNA viral loads were measured using the Abbott RealTime HIV-1 RT-PCR assay that do not amplify genomic regions present in lentiviral vectors contrary to the Roche Cobas PCR (our unpublished observations and De Ravin et al [27]). Due to the small volumes of plasma from the mice, a dilution was necessary to reach the volume needed for the assay. Thus, this detection limit varied between 200 and 2000 copies/mL depending on the

initial volume of mouse plasma.

Flow cytometry

Red blood cells from whole blood were lysed with 4.5 ml of water for 15 s before adding 0.5 ml of 10X PBS. Red blood cells from spleen or bone marrow were lysed with ACK buffer (NH_4Cl 0.15 M, KHCO3 10 mM, EDTA 0.1 mM). Cell suspensions were stained with an optimal quantity of antibodies at a concentration of 10^7 cells/mL in a final volume of 100 µL of PBS/FCS 3%. Incubation was performed in the dark at 6°C for 20 min. The following anti-human mAbs were used for cell surface staining: CD45 PE-CF594 (clone HI30; catalog number (cat ≠) 562279, BD Biosciences) anti-CCR5 Alexa Fluor 647 (HEK/1/85a; cat ≠ 313712, Biolegend), anti-CD4 PerCP (RPA-T4, cat ≠ 300528, Biolegend), anti-CD8 Alexa Fluor 700 (HIT8a, cat ≠ 300920, Biolegend), CD3 PE-Cy7 (UCHT1, cat≠ 300420, Biolegend). The human IgG1 mAb 2F5 specific for a gp41 epitope (cat ≠ AB001, Polymun, Austria) was used to detect the C46 peptide. The KC57-RD1 (cat≠ 6604667, Beckman Coulter) antibody was used to detect intracellular p24 after cells were treated with permeabilization buffer (eBioscience, fixation and permeabilization kit). All cell preparations were acquired on an LSRII cytometer (BD) and analyzed with FlowJo software (Tree Star, Portland, OR). The frequencies of positive cells were determined according to the fluorescence minus one (FMO) staining negative control.

Statistical analysis

No statistical method was used to assess sample size needed to detect an effect. Except for

the NSG/CD34 model, which is a single experiment, all the results shown in this study are compiled from 2 independent experiments. Two-tailed p values indicated on the graphs were calculated with Prism version 6.0 software (GraphPad Software, San Diego, CA), using the unpaired Mann-Whitney test with a confidence interval of 95%. The median value are indicated by horizontal bars on the graphs. Linear and non linear regression analysis were performed using Prism 6.0 to determine whether slopes significantly differed. Plateau with one phase decay association or dissociation equations were used to model the data.

Acknowledgments

This work was supported by grants from Agence Nationale de la Recherche to Guy Gorochov and Gilles Marodon. Nicolas Petit was supported by a doctoral fellowship from Fond Pierre Bergé /SIDAction and by the ANRS. The authors would like to thank David Klatzmann (INSERM U959, Paris, France) for his initial support on this project, Dorothée van Laer (Innsbruck University, Austria) for kind gift of the C46 peptide, Arnaud Moris (CIMI-PARIS, France) for the kind gift of NL-AD8 HIV-1 strain, Dr Hans Yssel (CIMI-PARIS) for performing Hoechst-based detection test of mycoplasma, Aude Burlion (CIMI-PARIS, France) for technical help. Nicolas Petit, Claude Baillou and Gilles Marodon performed experiments; Béatrice Levacher constructed the vectors; Corinne Amiel and Véronique Schneider performed HIV-1 qPCR; Karim Dorgham, Francois Lemoine, Guy Gorochov conceived experiments, contributed to essential reagents and corrected the manuscript; Nicolas Petit and Gilles Marodon conceived experiments, analyzed the data and wrote the manuscript.

Conflict of Interest

The authors declare no conflict of interest

Supplementary information is available at Gene Therapy's website

Figure S1. Survival and graft efficiency after ACT of activated and transduced T lymphocytes in NSG/PBL HuMice.

Figure S2. Selective advantage for LvGFP-C46-P2-modified $CD4^+$ cells is dependent on HIV-1 infection.

Figure S3. Resistance to HIV-1-induced deletion in LvGFP-C46-P2-injected NSG/PBL mice.

Figure S4. $CD4^+$ T cell deletion in LvGFP-control NSG/PBL mice.

Figure S5. Human cell reconstitution in 17 weeks-old in NSG/CD34 humanized mice.

References

1 Martinson JJ, Chapman NH, Rees DC, Liu YT, Clegg JB. Global distribution of the CCR5 gene 32-basepair deletion. *Nat Genet* 1997; **16**: 100–103.

2 Allers K, Hütter G, Hofmann J, Loddenkemper C, Rieger K, Thiel E *et al.* Evidence for the cure of HIV infection by CCR5Δ32/Δ32 stem cell transplantation. *Blood* 2011; **117**: 2791–9.

3 Holt N, Wang J, Kim K, Friedman G, Wang X, Taupin V *et al.* Human hematopoietic stem/progenitor cells modified by zinc-finger nucleases targeted to CCR5 control HIV-1 in vivo. *Nat Biotechnol* 2010; **28**: 839–847.

4 Didigu C a, Wilen CB, Wang J, Duong J, Secreto AJ, Danet-Desnoyers G a *et al.* Simultaneous zinc-finger nuclease editing of the HIV coreceptors ccr5 and cxcr4 protects CD4+ T cells from HIV-1 infection. *Blood* 2014; **123**: 61–9.

5 Perez EE, Wang J, Miller JC, Jouvenot Y, Kim KA, Liu O *et al.* Establishment of HIV-1 resistance in CD4+ T cells by genome editing using zinc-finger nucleases. *Nat Biotechnol* 2008; **26**: 808–816.

6 Tebas P, Stein D, Tang WW, Frank I, Wang SQ, Lee G *et al.* Gene Editing of CCR5 in Autologous CD4 T Cells of Persons Infected with HIV. *N Engl J Med* 2014; **370**: 901–910.

7 Peterson CW, Younan P, Jerome KR, Kiem H-P. Combinatorial anti-HIV gene therapy: using a multipronged approach to reach beyond HAART. *Gene Ther* 2013; **20**: 695–702.

8 Colin P, Bénureau Y, Staropoli I, Wang Y, Gonzalez N, Alcami J *et al.* HIV-1 exploits CCR5 conformational heterogeneity to escape inhibition by chemokines. *Proc Natl Acad Sci U S A* 2013; **110**: 9475–80.

9 Greenberg ML, Cammack N. Resistance to enfuvirtide, the first HIV fusion inhibitor. *J Antimicrob Chemother* 2004; **54**: 333–340.

10 Von Laer D, Hasselmann S, Hasselmann K. Gene therapy for HIV infection: what does it need to make it work? *J Gene Med* 2006; **8**: 658–667.

11 Doitsh G, Galloway NLK, Geng X, Yang Z, Monroe KM, Zepeda O *et al.* Cell death by pyroptosis drives CD4 T-cell depletion in HIV-1 infection. *Nature* 2014; **505**: 509–14.

12 Heredia A, Gilliam B, DeVico A, Le N, Bamba D, Flinko R *et al.* CCR5 density levels on primary CD4 T cells impact the replication and Enfuvirtide susceptibility of R5 HIV-1. *Aids* 2007; **21**: 1317–1322.

13 Anastassopoulou CG, Ketas TJ, Sanders RW, Klasse PJ, Moore JP. Effects of sequence changes in the HIV-1 gp41 fusion peptide on CCR5 inhibitor resistance. *Virology* 2012; **428**: 86–97.

14 Petit N, Dorgham K, Levacher B, Burlion A, Gorochov G, Marodon G. Targeting Both Viral and Host Determinants of Human Immunodeficiency Virus Entry, Using a New Lentiviral

Vector Coexpressing the T20 Fusion Inhibitor and a Selective CCL5 Intrakine. *Hum Gene Ther Methods* 2014; **25**: 232–40.

15 Hartley O, Dorgham K, Perez-Bercoff D, Cerini F, Heimann A, Gaertner H *et al.* Human immunodeficiency virus type 1 entry inhibitors selected on living cells from a library of phage chemokines. *J Virol* 2003; **77**: 6637–6644.

16 Schroers R, Davis CM, Wagner HJ, Chen SY. Lentiviral transduction of human T-lymphocytes with a RANTES intrakine inhibits human immunodeficiency virus type 1 infection. *Gene Ther* 2002; **9**: 889–897.

17 Egelhofer M, Brandenburg G, Martinius H, Schult-Dietrich P, Melikyan G, Kunert R *et al.* Inhibition of Human Immunodeficiency Virus Type 1 Entry in Cells Expressing gp41-Derived Peptides. *J Virol* 2004; **78**: 568–575.

18 Kimpel J, Braun SE, Qiu G, Wong FE, Conolle M, Schmitz JE *et al.* Survival of the Fittest: Positive Selection of CD4+ T Cells Expressing a Membrane-Bound Fusion Inhibitor Following HIV-1 Infection. *PLoS One* 2010; **5**: e12357.

19 Burke BP, Levin BR, Zhang J, Sahakyan A, Boyer J, Carroll M V *et al.* Engineering Cellular Resistance to HIV-1 Infection In Vivo Using a Dual Therapeutic Lentiviral Vector. *Mol Ther Acids* 2015; **4**: e236.

20 Trobridge GD, Wu RA, Beard BC, Chiu SY, Muñoz NM, von Laer D *et al.* Protection of stem cell-derived lymphocytes in a primate AIDS gene therapy model after in vivo selection. *PLoS One* 2009; **4**. doi:10.1371/journal.pone.0007693.

21 King MA, Covassin L, Brehm MA, Racki W, Pearson T, Leif J *et al.* Human peripheral blood leucocyte non-obese diabetic-severe combined immunodeficiency interleukin-2 receptor gamma chain gene mouse model of xenogeneic graft-versus-host-like disease and the role of host major histocompatibility complex. *Clin Exp Immunol* 2009; **157**: 104–118.

22 Younan PM, Polacino P, Kowalski JP, Peterson CW, Maurice NJ, Williams NP *et al.* Positive selection of mC46-expressing CD4+ T cells and maintenance of virus specific immunity in a primate AIDS model. *Blood* 2013; **122**: 179–187.

23 Shimizu S, Ringpis G-E, Marsden MD, Cortado R V, Wilhalme HM, Elashoff D *et al.* RNAi-Mediated CCR5 Knockdown Provides HIV-1 Resistance to Memory T Cells in Humanized BLT Mice. *Mol Ther Nucleic Acids* 2015; **4**: e227.

24 Myburgh R, Ivic S, Pepper MS, Gers-Huber G, Li D, Audigé A *et al.* Lentivector knock-down of CCR5 in hematopoietic stem cells confers functional and persistent HIV-1 resistance in humanized mice. *J Virol* 2015; **89**: 6761–6772.

25 Walker JE, Chen RX, McGee J, Nacey C, Pollard RB, Abedi M *et al.* Generation of an HIV-1-Resistant Immune System with CD34+ Hematopoietic Stem Cells Transduced with a Triple-Combination Anti-HIV Lentiviral Vector. J. Virol. 2012; **86**: 5719–5729.

26 Myburgh R, Ivic S, Pepper MS, Gers-Huber G, Li D, Audigé A *et al.* Lentivector knock-down of CCR5 in hematopoietic stem cells confers functional and persistent HIV-1 resistance in humanized mice. *J Virol* 2015; **89**: 6761–6772.

27 De Ravin SS, Gray JT, Throm RE, Spindler J, Kearney M, Wu X *et al.* False-Positive HIV PCR Test Following Ex Vivo Lentiviral Gene Transfer Treatment of X-linked Severe Combined Immunodeficiency Vector. *Mol Ther* 2014; **22**: 244–245.

28 Abarrategui-Pontes C, Créneguy A, Thinard R, Fine EJ, Thepenier V, Fournier LRL *et al.* Codon swapping of zinc finger nucleases confers expression in primary cells and in vivo from a single lentiviral vector. *Curr Gene Ther* 2014; **14**: 365–76.

29 DiGiusto DL, Krishnan A, Li L, Li H, Li S, Rao A *et al.* RNA-based gene therapy for HIV with lentiviral vector-modified CD34(+) cells in patients undergoing transplantation for AIDS-related lymphoma. *Sci Transl Med* 2010; **2**: 36ra43.

30 Podsakoff GM, Engel BC, Carbonaro DA, Choi C, Smogorzewska EM, Bauer G *et al.* Selective survival of peripheral blood lymphocytes in children with HIV-1 following delivery of an anti-HIV gene to bone marrow CD34+ cells. *Mol Ther* 2005; **12**: 77–86.

31 Zufferey R, Dull T, Mandel RJ, Bukovsky A, Quiroz D, Naldini L *et al.* Self-inactivating lentivirus vector for safe and efficient in vivo gene delivery. *J Virol* 1998; **98**: 9873–9880.

32 Marodon G, Mouly E, Blair EJ, Frisen C, Lemoine FM, Klatzmann D. Specific transgene expression in human and mouse CD4+ cells using lentiviral vectors with regulatory sequences from the CD4 gene. *Blood* 2003; **101**: 3416–3423.

Figure Legends

Figure 1. Lentiviral vector design and co-expression of anti-HIV-1 genes and eGFP into a lentiviral vector. (a) A schematic representation of the structure of the lentiviral vectors used in the present study is shown. (LTR: long terminal repeat; cppT: central polypurine tract of HIV-1; EF1α: Elongation factor 1 promoter; C46: membrane-bound form of T20 (C46 peptide); 2A: 2A sequence of the foot-and-mouth disease virus; P2i: P2-CCL5 intrakine; WPRE: Woodchuck Hepatitis virus regulatory element; ΔLTR: U3 deleted LTR). Indicated is the reference of the vector used throughout the study. Not to scale. **(b)** Co-expression of the C46 peptide (detected with the 2F5 mAb) and of eGFP and **(c)** co-expression of CCR5 and eGFP in human $CD4^+$ PBMC activated by CD3/CD28 beads and IL-2 21 to 29 days post transduction with the LvGFP-C46-P2 vector (NT: Non-transduced; FMO: fluorescence minus one; MFI: median fluorescence intensity) **(d)** *In vivo* CCR5 expression on $CD45^+CD3^+CD4^+$ T cells in GFP^+ and GFP^- cells from non-irradiated NSG mice grafted with 2.10^6 LvGFP-C46-P2 transduced T lymphocytes and analyzed in the blood and the spleen 34 to 53 days post-graft.

Figure 2. Protection of genetically-modified human $CD4^+$ T cells from HIV-1 infection in NSG/PBL mice. (a-b) Frequencies of GFP^+ cells in human $CD45^+CD3^+CD4^+$ T cells in the blood at various days after HIV-1 infection **(a)** and in the spleen or bone marrow (BM) **(b)** 35 to 45 days after injection of LvGFP- or LvGFP-C46-P2-modified T cells in NSG mice. **(c)** Representative histograms and dot plots showing the gating strategy to determine the frequencies of $CD4^+$ T cells in GFP^+ and GFP^- human $CD3^+$ T cells. **(d-e)** Frequencies of $CD4^+$ cells in the $CD3^+GFP^+$ and $CD3^+GFP^-$ populations were determined in LvGFP-C46-P2-injected mice in the blood at various days after infection **(d)** and in the spleen or bone marrow (BM) **(e)** at the end of the experiment. The results are compiled from 2 independent experiments using the P3 ACT protocol (Fig. S1). Non linear regression analysis curve fit are shown. The p value indicate the significant difference between the two slopes.

Figure 3. Resistance of genetically-modified $CD4^+$ T cells to HIV-1-induced depletion *in vivo* in NSG/CD34 HuMice. (a) Blood frequencies of $CD4^+$ cells in $CD3^+GFP^+$ or $CD3^+GFP^-$

populations were determined in non-infected (HIV^-) or **(b)** infected **(**HIV^+) NSG HuMice at various time points after infection. Linear regression curve fit and p values are depicted on the graphs. n.s = not significant ($p>0.05$) **(c)** Frequencies of $CD4^+$ cells into $CD3^+GFP^+$ or $CD3^+GFP^-$ populations in HIV^- or **(d)** HIV^+ mice in the spleen, the lymph nodes (LN) and the bone marrow (BM) 11 weeks post-infection.

Figure 4. Gene transfer of entry inhibitors impacts viral replication in NSG/CD34 HuMice **(a)** Viral load was measured by qPCR after HIV-1 infection in LvGFP-C46-P2-treated mice with undetectable (-GFP) or detectable GFP^+ cells (+GFP) in $CD4^+$ T cells prior to infection. Shown is the viral load value normalized by the frequency of human $CD45^+CD3^+CD4^+$ T cells present in total cells of the blood sample for each time point. **(b)** Frequencies of $p24^+$ cells in $CD4^+$ T cells from the lymph node of NSG HuMice with (+GFP) or without GFP^+ cells (-GFP) 77 days after infection with NL-AD8 HIV-1 (HIV+) or non infected (HIV-). A representative CD4 vs p24 staining is shown above each group. One mouse from the (+GFP) group was excluded from the graph since it did not show any protection against HIV-1-induced depletion in the periphery.

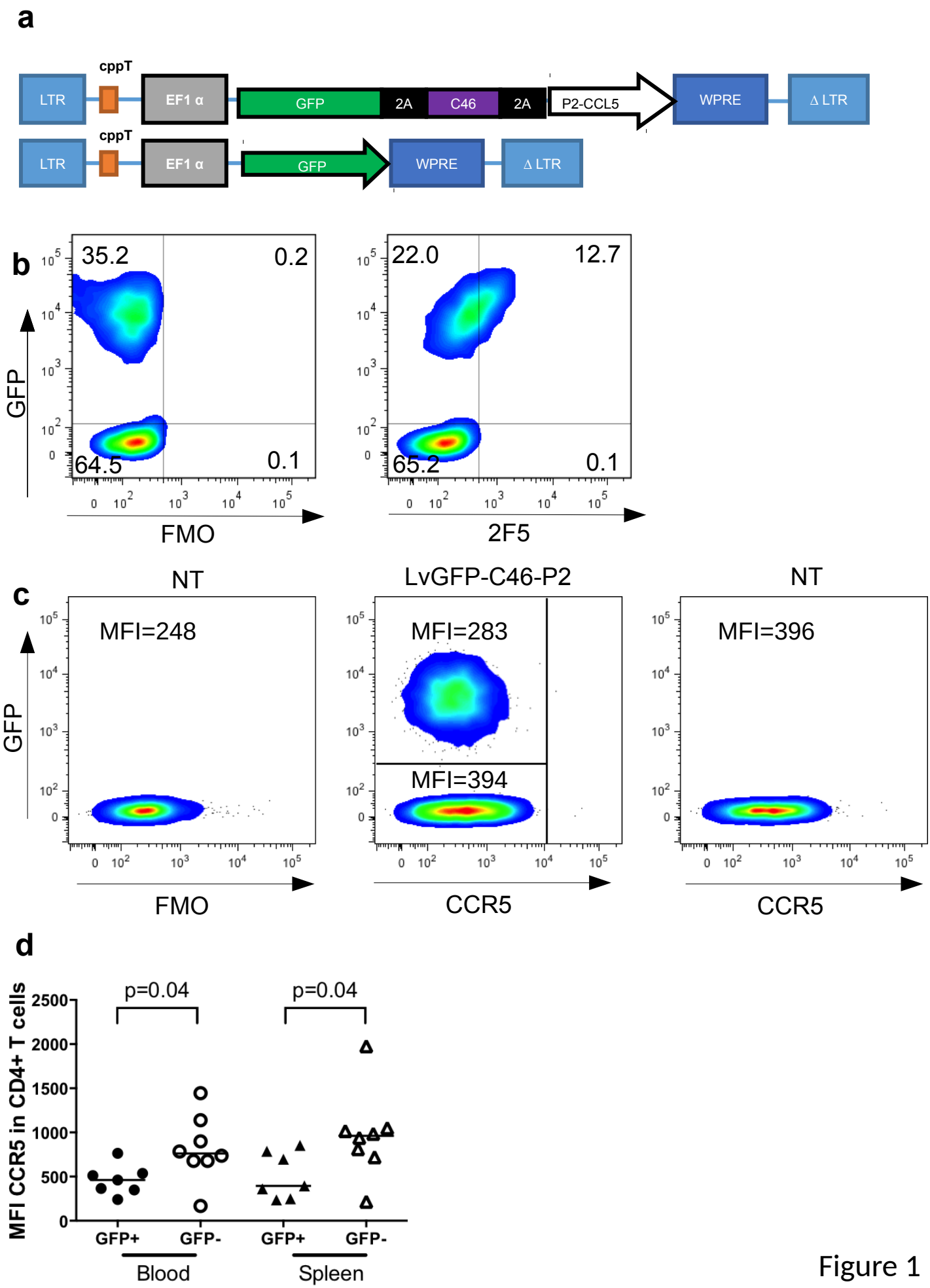
a
cppT
LTR
EF1 α
GFP
2A
C46
2A
P2-CCL5
WPRE
Δ LTR
cppT
LTR
EF1 α
GFP
WPRE
Δ LTR
b
35.2
0.2
64.5
0.1
GFP
FMO
22.0
12.7
65.2
0.1
2F5
c
NT
MFI=248
GFP
FMO
LvGFP-C46-P2
MFI=283
MFI=394
CCR5
NT
MFI=396
CCR5
d
MFI CCR5 in CD4+ T cells
p=0.04
p=0.04
GFP+
GFP-
GFP+
GFP-
Blood
Spleen

Figure 1

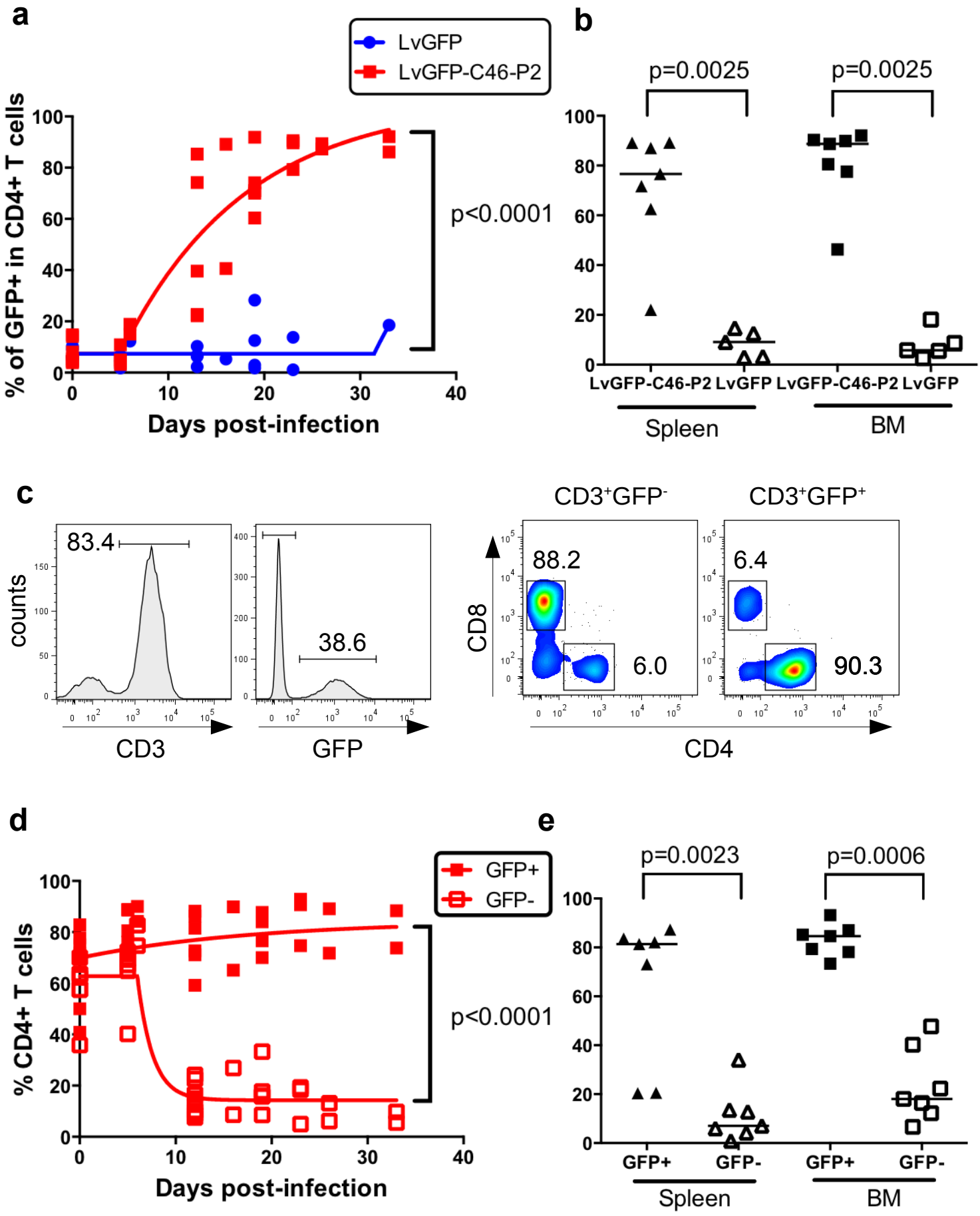
a
LvGFP
LvGFP-C46-P2
% of GFP+ in CD4+ T cells
Days post-infection
p<0.0001
b
p=0.0025
p=0.0025
LvGFP-C46-P2 LvGFP LvGFP-C46-P2 LvGFP
Spleen
BM
c
CD3+GFP-
CD3+GFP+
83.4
38.6
counts
CD3
GFP
88.2
6.0
6.4
90.3
CD8
CD4
d
GFP+
GFP-
% CD4+ T cells
Days post-infection
p<0.0001
e
p=0.0023
p=0.0006
GFP+
GFP-
GFP+
GFP-
Spleen
BM

Figure 2

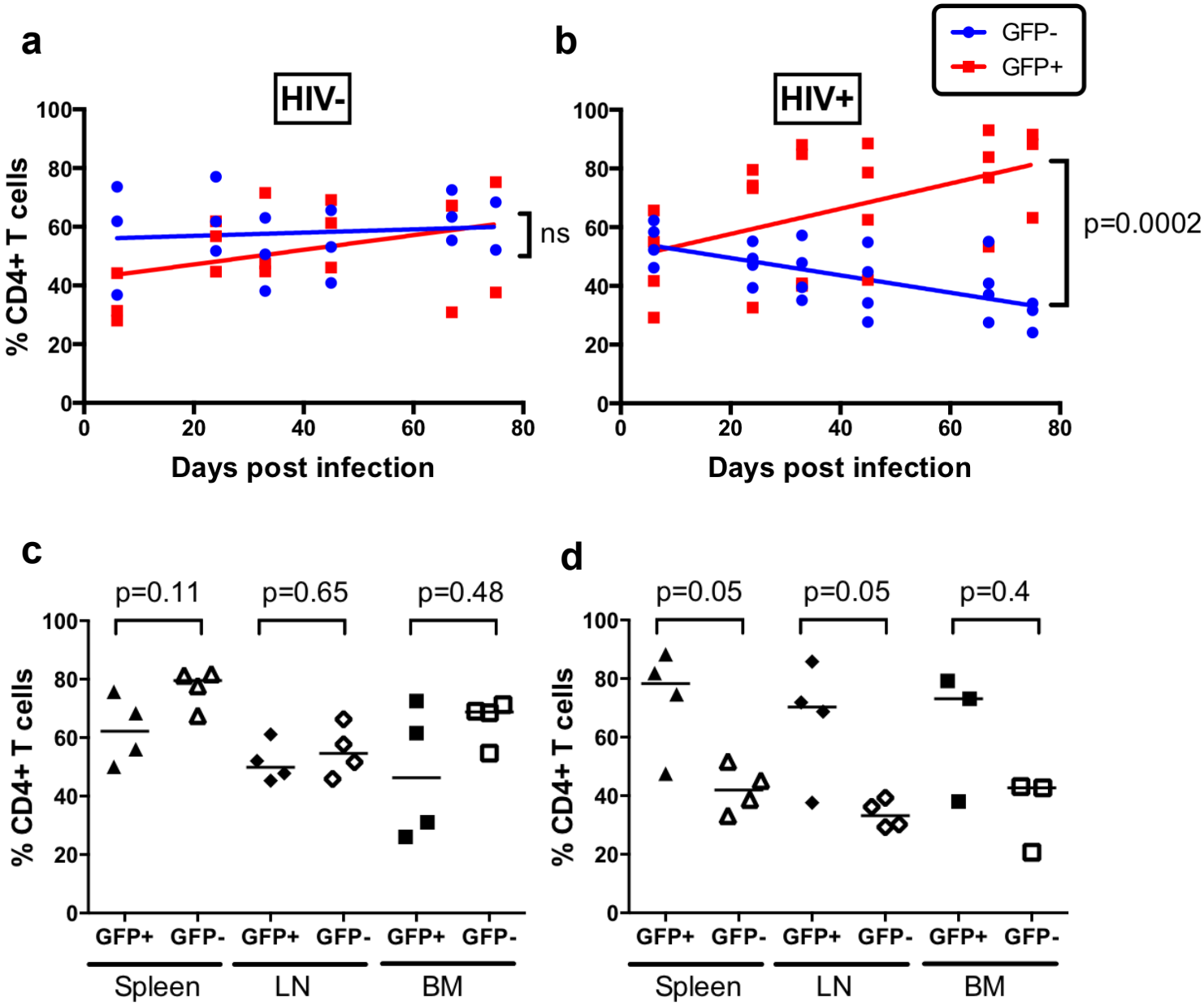
a
HIV-
% CD4+ T cells
Days post infection
ns
b
HIV+
GFP-
GFP+
p=0.0002
c
p=0.11
p=0.65
p=0.48
GFP+ GFP- GFP+ GFP- GFP+ GFP-
Spleen
LN
BM
d
p=0.05
p=0.05
p=0.4

Figure 3

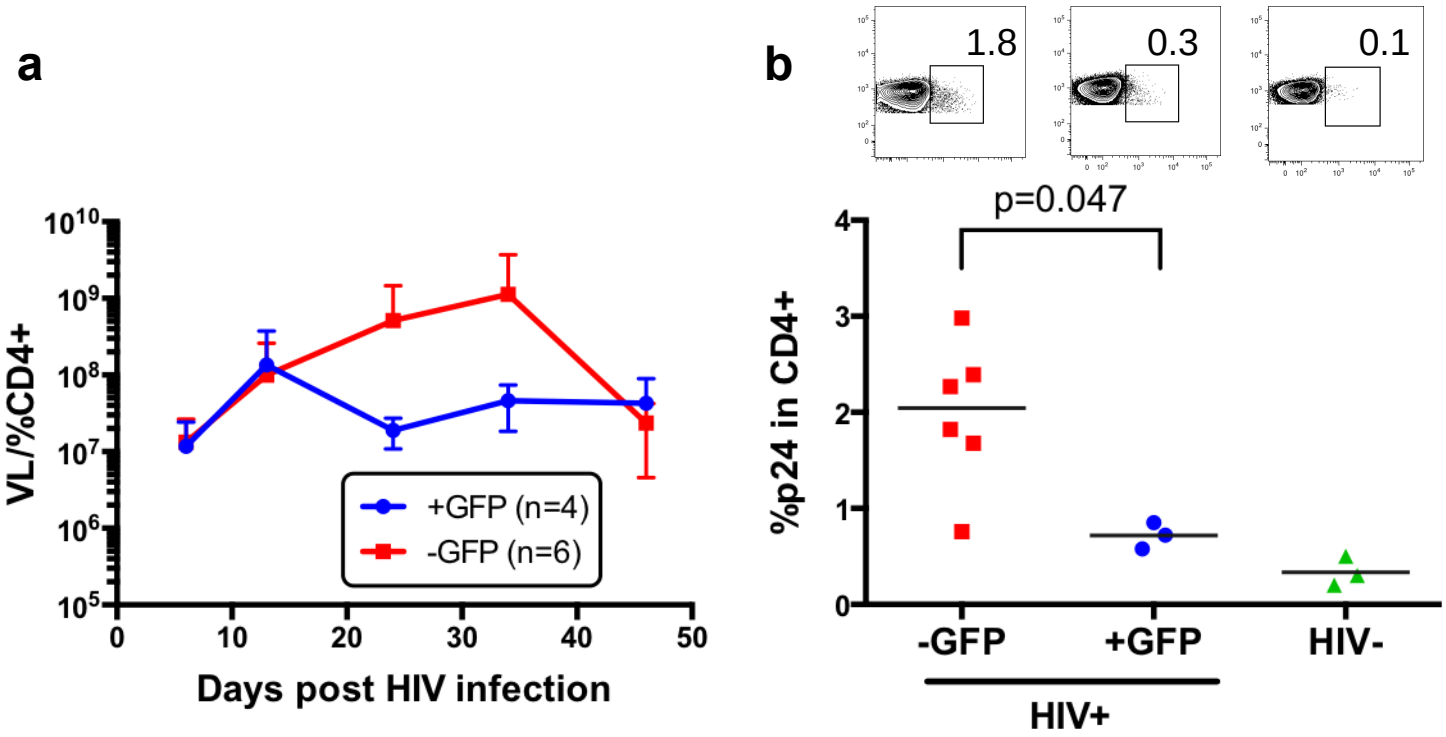
a
b
1.8
0.3
0.1
p=0.047
VL/%CD4+
Days post HIV infection
+GFP (n=4)
-GFP (n=6)
%p24 in CD4+
-GFP
+GFP
HIV-
HIV+

Figure 4